OPECAL

D12:ATBD
RADIOMETRY MONITORING USING DESERT SITE

TECHNICAL NOTE

	Name	Company	Date	Signature
Prepared by :	B. Berthelot	Magellium	23/01/2020	
Checked by :		Magellium		
Approved by :	B. Berthelot	Magellium	23/01/2020	

Document reference :	OPECAL-TN-043-MAG
Issue.Revision :	2.0
Date :	16/12/2019
Client :	ESTEC
Ref., Tender :	AO/1-7043/11/F/MOS

Distribution list

	Name	Company	N. copies
Addresses :	M. Bouvet	ESA/ESTEC	1
Internal copy :	Customer file Project Manager Development team	Magellium Magellium Magellium	1 (digital) 1 (digital) 1 (digital)

Document Change Record

Iss.	Rev.	Date	Reason	Comments
1	0	02/11/2014	Creation of the document	
1	1	03/12/2014	Answers to ESA comments	
1	2	28/01/2015	Answers to ESA comments v2	Section 3.2.2.5 (RTM Solar Irradiance correction) removed Results updated Budget error rewritten Typo corrections
2	0	19/11/2019	Section 3.2.3.2 (Filtered BRDF) has been removed and replaced by BRDF climatology	
			Spectral correction has been added.	

Table of contents

List of the Tables

List of the Figures

1 Objectives of the document

The purpose of this study is to develop and implement a method to monitor sensor radiometry of optical sensors using desert site into DIMITRI software.

1.1 Related documents

1.1.1 Applicable documents

Table 1-1: List of applicable documents

Id.	Ref.	Description
AD1	QA4EO-QAEO-GEN-DQK-001/7, Version 4.0	QA4EO Guidelines (seven documents) http://qa4eo.org/
AD2	OPECAL-TN-043-MAG-Desert-v1.2	ATBD radiometric sensor radiometry using Desert site, B. Berthelot, 2015.
AD3	SOW	

1.1.2 Reference documents

Table 1-2: List of reference documents

Id.	Ref.
RD 1.	Bouvet M. , Ramoino F., Radiometric intercomparison of AATSR, MERIS, and Aqua MODIS over Dome Concordia (Antarctica), Can. J. Remote Sensing, Vol. 36, No. 5, pp. 464–473, 2010. http://pubs.casi.ca/loi/cjrs
RD 2.	DIMITRI Software User Manual ftp://ftp.estec.esa.int/pub/gsp/anonymous/Earth_Observation_Multi-mission_Phase-E2_Operational_Calibration/DIMITRI_SUM.pdf
RD 3.	DIMITRI Software Design Document ftp://ftp.estec.esa.int/pub/gsp/anonymous/Earth_Observation_Multi-mission_Phase-E2_Operational_Calibration/DIMITRI_SDD.pdf
RD 4.	Statement of Word GSP activity 'Towards the Intercalibration of EO Medium Resolution Multi-Spectral Imagers' ftp://ftp.estec.esa.int/pub/gsp/anonymous/Earth_Observation_Multi-mission_Phase-E2_Operational_Calibration/SoW_GSP_TowardsTheIntercomparisonOfEOMediumResolutionMultiSpectralImagers.pdf
RD 5.	Hagolle et Al., Results of POLDER in-flight Calibration, IEEE Transactions on Geoscience and Remote Sensing, May 1999, Volume 37, Number 03 [p. 1550]. http://ieeexplore.ieee.org/xpl/RecentIssue.jsp?punumber=36

RD 6.	Vermote, E., R. Santer, P.Y. Deschamps and M. Herman, In-flight Calibration of Large Field-of-View Sensors at Short Wavelengths using Rayleigh Scattering, Int. Journal of Remote Sensing, 13, No 18, 1992. http://www.tandf.co.uk/journals/tres
RD 7.	Smith D., Poulsen C., Latter B.: Calibration Status of the AATSR Reflectance Channels, MERIS AATSR workshop 2008 proceedings. http://earth.esa.int/meris_aatsr_2008/

1.1.3 Bibliography

- Ackerman, S. A., K. I. Strabala, W. P. Menzel, R. A. Frey, C. C.Moeller, and L. E. Gumley, 1998: Discriminating clear-sky from clouds with MODIS. J. Geophys. Res., 103 (D24), 32 141–32 157.
- Berthelot, B.; Dedieu, G., "Operational method to correct VEGETATION satellite measurements from atmospheric effects," *Geoscience and Remote Sensing Symposium, 2000. Proceedings. IGARSS 2000. IEEE 2000 International* , vol.2, no., pp.831,833 vol.2, 2000
- Holben, B. N., Kaufman, Y. J., and Kendall, J. D., 1990, NOAA-11 AVHRR visible and near-IR inflight calibration: The International Journal of Remote Sensing, 11, 1511-1519.
- Kaufman Y.J., and B. N. Holben (1993). Calibration of the AVHRR visible and Near-IR bands by atmospheric scattering, ocean glint and desert reflection *Int. J. Rem. Sens.*, *14*, 21-52Cosnefroy et al., 1996,
- Kotchenova S.Y. & and E.F. Vermote, Validation of a vector version of the 6S radiative transfer code for atmospheric correction of satellite data. Part II: Homogeneous Lambertian and anisotropic surfaces, Applied Optics, 2007.
- Kotchenova, S.Y., E.F. Vermote, R. Matarrese, & F.J. Klemm, Jr., Validation of a vector version of the 6S radiative transfer code for atmospheric correction of satellite data. Part I: Path Radiance, Applied Optics, 45(26), 6726-6774, 2006.
- Li, X. and Strahler, A.H. 1992.Geometric-optical bidirectional reflectance modeling of the discrete crown vegetation canopy: Effect of crown shape and mutual shadowing. IEEE, Transactions on Geoscience and Remote Sensing, Vol. 30, pp. 276-292.
- Morel, A. Optical modeling of the upper ocean in relation to its biogenous matter content (case I waters), Journal of Geophysical Research, 93(C9), 10749-10768, 1988.
- Rahman and Dedieu, 1994; SMAC: a simplified method for the atmospheric correction of satellite measurements in the solar spectrum", Int. J. Remote Sensing, 1994, vol.15, no.1, 123-143.
- Berthelot and Dedieu, 2000, Operational method to correct vegetation satellite measurements from atmospheric effects. IGARSS'00.
- Ross, J.K. (1981). The radiation regime and architecture of plant stands, Dr W Junk, The Hague.
- Schaaf, CB, Gao, F, Strahler, AH, Lucht, W, Li, XW, Tsang, T, Strugnell, NC, Zhang, XY, Jin, YF, Muller, JP, Lewis, P, Barnsley, M, Hobson, P, Disney, M, Roberts, G, Dunderdale, M, Doll, C, d'Entremont, RP, Hu, BX, Liang, SL, Privette, JL, Roy, D (2002). "First operational BRDF, albedo nadir reflectance products from MODIS". Remote Sensing of environment, 83(2-Jan), 135-148.
- Bouvet, M., Radiometric comparison of multispectral imagers over a pseudo-invariant calibration site using a reference radiometric model, Remote Sensing of Environment, 140 (2014) 141–154.

Berthelot, B., 2001, Estimation of SMAC coefficients for optical sensors, CNES report.

1.1.4 Acronyms

6SV	Second Simulation of a Satellite Signal in the Solar Spectrum, Vector
AATSR	Advanced Along Track Scanning Radiometer
ADEOS	Advanced Earth Observation Satellite
AERONET	AErosol RObotic NETwork
ASTR	Along Track Scanning Radiometer
BRDF	Bidirectional Reflectance Distribution Function
Cal/Val	CALibration and VALidation
CEOS	Committee on Earth Observation Satellites
CNES	Centre National d'Etudes Spatiales
DIMITRI	Database for Imaging Multispectral Instruments and Tools for Radiometric Intercomparison
DN	Digital Number
DTM	Digital Terrain Model
ENVISAT	ENVIronment SATellite
EO	Earth Observation
ESA	European Space Agency
EUMETSAT	European Organisation for the Exploitation of Meteorological Satellites
GSICS	Global Space-based Inter-calibration System
IVOS	Infrared and Visible Optical Sensors
MERIS	Medium Resolution Imaging Spectrometer
MISR	Multi-angle Imaging SpectroRadiometer
MODIS	Moderate Resolution Imaging Spectroradiometer
NASA	National Aeronautics and Space Administration
NOAA	National Oceanic and Atmospheric Administration
OLCI	Ocean and Land Color Instrument
PARASOL	Polarization & Anisotropy of Reflectances for Atmospheric Sciences coupled with Observations from a Lidar
POLDER	POLarization and Directionality of the Earth's Reflectances
QA4EO	Quality Assurance Framework for Earth Observation
RADTRAN	Radiative Transfer
RIM	Radiometric Instrument Model
RTM	Radiative Transfer Model
SADE	Structure d'Accueil de Données d'Etalonnage
SWIR	Short Wave Infra-Red
TOA	Top Of Atmosphere
VGT	VEGETATION
VIS	VISible
WG	Working Group
WGCG	Working Group on Calibration and Validation

2 Introduction

This document is an update of the Algorithm Theoretical Basis Document described in AD2. Following recommendations and possible improvements listed in the first version of the ATBD, an update of the algorithm has been performed. It concerns the assessment of the BRDF correction and the introduction of a spectral correction.

As it is described in the version 1 of the ATBD, this document reports sources of input data, both satellite and auxiliary data. It provides the physical theory and mathematical background underlying the use of this information in the method. It includes implementation details, and describes assumptions and limitations of the adopted approach.

This task is referred by WP 300 of the SOW (AD.3).

Section 3 details the method and its implementation. The updates are identified. Results obtained for MERIS are given in section 4. Section 5 recaps the uncertainty of the method.

3 Algorithm overview

3.1 Principle of the method

The deserts are stable targets that are used for a long time for monitoring the radiometric stability of sensors on board satellite. Their temporal instability without atmospheric correction has been determined to be less than 1–2% over a year.

A list of selected sites has been identified in Sahara desert by several calibration teams; Holben et al., 1990; Kaufman and Holben, 1993; Cosnefroy et al., 1996, for instance. The reference list of Cosnefroy et al., 1996 accounts for 20 sites. Selection has been performed using Meteosat-4 data for the period July 1989–January 1990 to identify 100×100 km^2 areas with a relative spatial uniformity of less than 3%. These sites are monitored for more than 20 years and there characteristics have been described in terms of spectral and temporal variability.

Desert sites are large sites (1° x 1°). Among the 20 sites, one located in Libya is endorsed by the CEOS. The site is named Libya 4. Its location is [28.05 29.05E, 22.89-23.89 N]. The site is composed of dunes at multiple scales as it can be seen on the figure below.

Figure 3-1: Libya 4 site seen by ETM (ETM+ Bands 321), source USGS.

The stability of the surface reflectance is the property that is used for developing the method. As the site is radiometrically stable, any change in the reflectance is attributed to the temporal change of the instrument's sensitivity.

Furthermore, these sites have been used to intercalibrate different sensors. But the method is not implemented in the frame of the project.

The principle of the method is to compare the measurements provided by the sensor above the desert site to a simulation of the top-of-atmosphere reflectance (Eq. 1). This ratio is computed

for all acquisitions and monitored on a large period of time to detect possible change in sensor radiometry.

$$\Delta\rho = \frac{\rho_{TOA}^{Measured}}{\rho_{TOA}^{Simulated}} \quad \textbf{Eq. 1}$$

In this ATBD, we will describe the method implemented to monitor the temporal variability of this ratio.

3.1.1 Method

3.1.1.1 Stability monitoring

Desert calibration method relies on the comparison between TOA reflectances (corrected for gaseous absorption) measured by the sensors available in DIMITRI database and the modelled TOA reflectances. The desert calibration is based on the monitoring of the stability of ρ_{toa}. A surface model is coupled to the atmosphere to simulate the TOA reflectance using RTM.

Let's call $\rho_{TOA}^{Measured*}$ the apparent Top Of Atmosphere reflectance, and $\rho_{TOA}^{Measured}$ the TOA reflectance.

The apparent TOA reflectance, normalised to the gaseous transmission, is modelled by the following expression:

$$\rho_{toa} = \rho_{atm} + \frac{T_{atm}^{\downarrow}\rho_g T_{atm}^{\uparrow}}{(1 - s_{atm}\rho_s)} \quad \textbf{Eq. 2}$$

and

$$\rho_{TOA}^{Measured} = \frac{\rho_{TOA}^{Measured*}}{Tg} \quad \textbf{Eq. 3}$$

where ρ_{atm} is the reflectance due to molecular and aerosol scattering ρ_g is the ground reflectance), $T_{atm}^{\uparrow}T_{atm}^{\downarrow}$ is the product of the total transmittances of molecules and aerosols, respectively, along the path Sun to surface and surface to satellite, s is the atmospheric albedo.

The comparison of the modelled to the measured reflectance over time provided the assessment of the sensor radiometry.

In the method, the TOA reflectance values are estimated using the SMAC method (Rahman and Dedieu, 1994; Berthelot and Dedieu, 2000). The input of the SMAC method is the same as the input of the 6SV radiative transfer code (Kotchenova et al., 2006).

In this case, simulated TOA reflectances values are determined by three types of factors:

- surface properties

  The surface properties of desert sites are described with a BRDF model. Several models are available.
- atmospheric conditions

  Aerosol loadings are unknown. A mean value is be used.
- Observation conditions including solar zenith angle, view zenith angle and relative azimuth angle.

As SMAC is an analytical method, the comparison of the measured TOA against the simulated one is fast. The evaluation of the sensor radiometry is defined by the ratio of the measured reflectance over the estimated one (Eq. 1).

3.1.1.2 Multitemporal monitoring

The goal of multi-temporal calibration is to monitor the stability and variations of the sensors responses over time. The temporal variations of the measured to simulated TOA reflectance ratio are monitored regularly against time for a long period. A function is fitted to estimate the variability against time.

3.1.2 Modelling

3.1.2.1 SMAC

SMAC (Simplified Method for Atmospheric Correction) initially developed by Rahman and Dedieu (1994) is a method which allows correcting atmospheric effects of satellite data time series based on 5S radiative transfer model. The method has been upgraded by Berthelot and Dedieu (1997) based on 6Sv41 radiative transfer model and used for the correction of atmospheric effects of VEGETATION data in an operational processing line (at CTIV). It is also added as a processor in the ESA BEAM toolbox to correct MERIS L1B data from atmospheric effects over land.

The atmospheric parameters are estimated using a set of equations which described analytically the absorption and scattering of molecules and aerosols in the atmosphere. The code is generic. Only the set of coefficients applied on these equations is depending on the spectral band. These coefficients are computed for a selected type of aerosol and one type of atmosphere.

The performance of SMAC/6S atmospheric reflectance estimation has been evaluated by computing the root mean square error (rmse) and the maximum absolute or relative error with respect to the 6S reference for SMAC. More than 50.000 simulations including extreme variations of the input parameters have been made to get the following results.

The root mean square error (rmse) is used to assess the performance of the method. It is expressed in reflectance unit. Rmse in blue band is around 0.007. It decreases to 0.002 in the NIR bands, and 0.001 in the SWIR.

3.1.2.2 BRDF

The surface properties of Libya4 site are described with a BRDF model. We choose to model the bidirectional reflectance of the surface using a reflectance model developed by MODIS team (Schaaf et al., 2002). The MODIS BRDF/Albedo algorithm is a linear BRDF model which relies on the weighted sum of an isotropic parameter and two functions (or kernels) of viewing and illumination geometry to determine reflectance. One of these kernels, $K_{vol}(\theta_s, \theta_v, \phi,\lambda)$, is derived from volume scattering radiative transfer models (Ross, 1981) and the other, $K_{geo}(\theta_s, \theta_v, \phi,\lambda)$, from surface scattering and geometric shadow casting theory (Li and Strahler, 1992).

$$R(\theta_s, \theta_v, \phi, \lambda)= f_{iso}(\lambda)+f_{vol}. K_{vol}(\theta_s, \theta_v, \phi,\lambda) + f_{geo}. K_{geo}(\theta_s, \theta_v, \phi,\lambda) \qquad \textit{Eq. 4}$$

The MODIS BRDF/albedo product provides with the three coefficients used to estimate the surface reflectance. f_{iso}, f_{vol} and f_{geo} parameters are referred by K1, K2, K3 in the following.

3.1.2.2.1 KERNEL description

The BRDF model kernel K_{vol} (also called RossThick kernel) is given by:

$$K_{vol}(\theta_s,\theta_s,d\phi)=\frac{(\pi/2-\xi)\cos\xi+\sin\xi}{\cos(\theta_s)+\cos(\theta_v)}-\frac{\pi}{4} \qquad \textbf{Eq. 5}$$

Where ξ is the scattering angle, given by

$$\cos\xi=\cos(\theta_s)\cos(\theta_v)+\sin(\theta_s)\sin(\theta_v)\cos d\phi \qquad \textbf{Eq. 6}$$

The BRDF model kernel K_{geo} (also called LiSparse kernel) is given by:

$$K_{geo}(\theta_s,\theta_v,d\phi)=O(\theta_s,\theta_v,d\phi)-\sec(\theta_s)-\sec(\theta_v)+\frac{1}{2}(1+\cos(\xi))\sec(\theta_s)\sec(\theta_v) \qquad \textbf{Eq. 7}$$

Where

$$O(\theta_s,\theta_v,d\phi)=\frac{1}{\pi}(t-\sin t\cos t)(\sec(\theta_s)+\sec(\theta_v)) \qquad \textbf{Eq. 8}$$

With

$$\cos t=\frac{2\sqrt{D^2+(tg(\theta_s)tg(\theta_v)\sin(d\phi))^2}}{\sec(\theta_s)+\sec(\theta_v)} \qquad \textbf{Eq. 9}$$

And with

$$D=\sqrt{tg^2(\theta_s)+tg^2(\theta_v)-2tg(\theta_s)tg(\theta_v)\cos(d\phi)} \qquad \textbf{Eq. 10}$$

3.1.2.2.2 MCD43B1 product description

The MODIS BRDF/Albedo Model Parameters product (Collection 5, MCD43B1) contains three-dimensional (3D) data sets providing users with weighting parameters for the anisotropy models used to derive the Albedo and BRDF products. The models support the spatial relationship and parameter characterization best describing the differences in radiation due to the scattering (anisotropy) of each pixel, relying on multi-date, atmospherically corrected, cloud-cleared input data measured over 16-day periods (Source MODIS).

Both Terra and Aqua data are used in the generation of this product, providing the highest probability for quality input data and designating it as an MCD, meaning Combined, product.

Data are available at 1km, which is an average of the 500m values. The products are produced every 8 days with 16 days of acquisition (i.e., production period 2001001 includes acquisition between Days 001 and 016, production period 2001009 includes acquisition between Days 009 and 024). 46 products are available per year.

MCD43B1 product supply spectral MODIS channels 1–7 BRDF model parameters used to reconstruct the entire surface BRDF and compute the directional reflectance at any view or solar zenith angle desired.

Coefficients have been extracted over Libya 4 from 2001 to 2016. An example is reported in the figure below for all bands.

Table 3-1: MODIS spectral band order

Band	Bandwidth (nm)
1	620 - 670
2	841 - 876
3	459 - 479
4	545 - 565
5	1230 - 1250
6	1628 - 1652
7	2105 - 2155

The spatial, variability of each coefficient in all MODIS band is represented hereafter for one date (2011, Julian day 180).

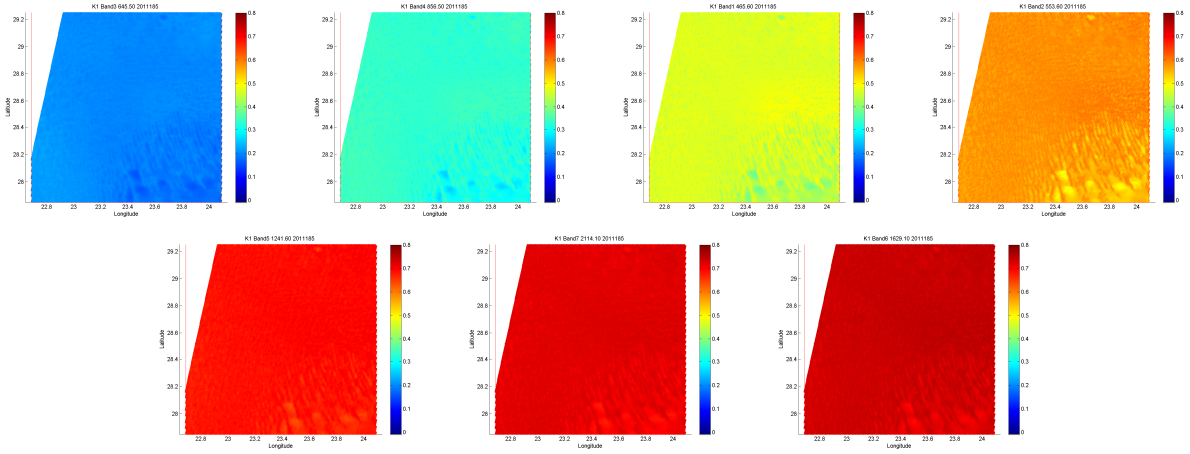

Figure 3-2: K1 coefficient- Synthesis of June, Julian day 180, 2011

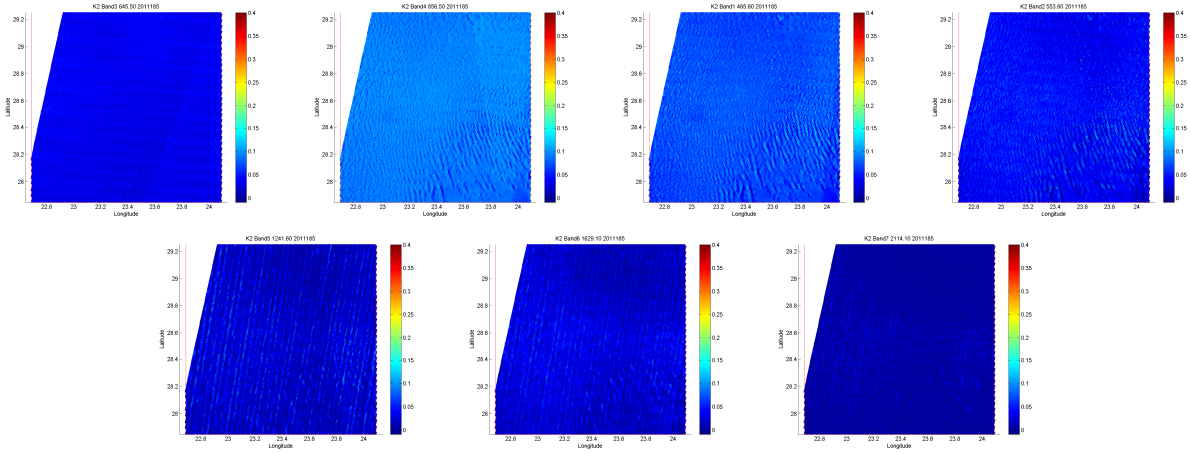

Figure 3-3: K2 coefficient- Synthesis of June, Julian day 180, 2011

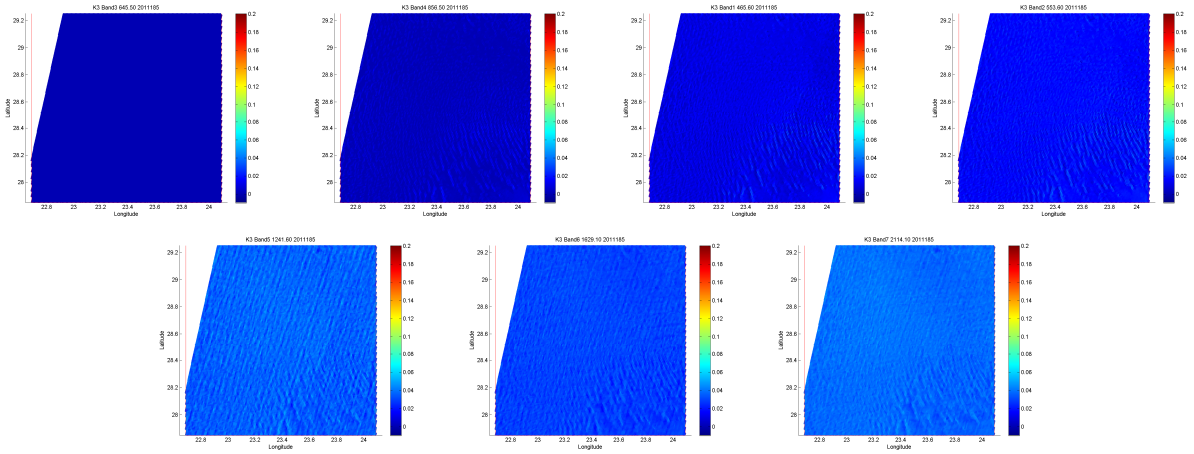

Figure 3-4: K3 coefficient- Synthesis of June, Julian day 180, 2011

3.1.2.3 Atmosphere characteristics

The desert aerosol model is used with an aerosol optical thickness set to 0.1 at 550 nm.

3.2 Implementation description

3.2.1 Overall steps

This paragraph provides with the overall steps that have to be done to estimate the ratio of measured to simulated reflectance.

1) Read the database and select images acquired in the desert site.

   For each selected date (loop)

2) Read the TOA reflectances of clear pixels acquired into the site footprint for the selected date.
3) Read auxiliary data
   - 3.1) Water vapour content
   - 3.2) Ozone content
4) Check Pixels selection test
   - 4.1) Select valid pixels
   - 4.2) Select clear pixels
   - 4.3) Select scenes for which cloud coverage is less than 20%
5) Correct the measured TOA reflectances from gaseous absorption
6) Read BRDF model coefficients from Climatology, interpolated at the date of the acquisition in the 7 MODIS bands
7) Simulate the BRDF in MODIS band for the geometry of the sensor
8) For all sensors except MODIS
   - 8.1) Interpolate spectrally the surface reflectance for the spectral band of the sensor

9) Estimate the TOA reflectance corrected from Tg in the sensor bands using SMAC

10) Estimate the reflectance ratio $\Delta\rho = \frac{\rho_{TOA}^{Measured}}{\rho_{TOA}^{Simulated}}$ in the all bands

3.2.2 Detailed steps

3.2.2.1 Input data selection

DIMITRI data ingestion module allows to extract for each acquisition the area which contains the desert site. One file is written for one acquisition. According to the period selected by the user, these files are read and used as input of the method.

The output file of the ingestion module contains the following information:

- Latitude;
- Longitude;
- Zenith and azimuth solar angles;
- Zenith and azimuth view angles;
- TOA reflectances in all channels;
- Cloud mask;

3.2.2.2 Auxiliary data extraction

Water vapour content, ozone content and pressure are extracted from ERA dataset for the location of the site. The data are provided each 6 hours. A linear interpolation is performed to estimate the different content at the hour of acquisition.

3.2.2.3 Pixel selection

The selection of pixels is the first step of the processing. The selection checks that there are:

- Valid pixels;
- Clear pixels;
- Less than 20% of clouds in the site.

If the following criteria are not validated, the method is not applied.

3.2.2.4 Correction of the apparent TOA reflectance from gaseous transmission

The comparison of the measured reflectance to the estimated one is performed on apparent TOA reflectances corrected from the gaseous transmission. Therefore, it is necessary to estimate the gaseous transmission for each pixel selected by the previous selection step.

The gaseous transmission has been estimated using SMAC formulation.

Analytical formulation is used to simulate the gaseous transmission from the air mass, gaz content (water vapour content, ozone content) and surface pressure. The formulation has been developed first by Rahman and Dedieu, (1996), then improved by Berthelot and Dedieu (2000). SMAC coefficient database has been developed for all optical sensors on orbit up to 2008 by B. Berthelot and is made available for free on CESBIO web site. The coefficients are estimated for H_20, O_3, O_2, CO_2, CH_4, NO_2, CO gaz.

- Input for total gaseous transmission estimation is :

- Solar zenith angle
- View zenith angle
- Water vapour content
- Ozone content
- Pressure
- SMAC coefficients for all bands

Output is :

- Total Gazeous transmission.

3.2.2.5 Read BRDF model coefficients interpolated at the date of the acquisition in the 7 MODIS bands

The BRDF coefficients are taken from the climatology of the MODIS BRDF product. The 21 coefficients (3 K x 7 spectral bands) are interpolated linearly at the date of acquisition from the product.

3.2.2.6 Simulate the BRDF in the 7 MODIS bands for the geometry of the sensor

The BRDF is computed using the three coefficients and the model in the geometry configuration of the acquisition.

3.2.2.7 Spectral interpolation

This step is applied only for all sensors except MODIS.

The surface reflectance is interpolated in the spectral bands of the sensor using the MODIS surface reflectance estimated in the previous step. As the MODIS spectral bands are spaced from each other by several tens of nanometers, they could not reproduce the real spectral shape of the surface reflectance, such as it could be measured with a spectro radiometer.

Therefore, a hyperspectral sand spectra which has this spectral variability is used to improve the spectral interpolation. This spectrum is slightly adapted to have the same values of MODIS reflectances.

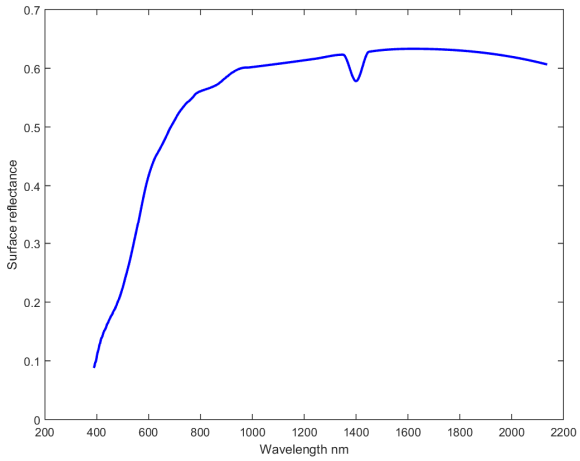

Figure 3-5: Hyperspectral spectrum

3.2.2.8 TOA reflectance estimation

The SMAC method is used to simulate the TOA reflectance (normalised to the gaseous transmission) using the atmosphere characteristics and the solar and view geometry of the acquisition.

3.2.2.9 Δρ estimation in the all bands

The ratio of measured TOA reflectances out to simulated TOA reflectances is computed for all the bands.

$$\Delta\rho = \frac{\rho_{toa}^{measured}}{\rho_{toa}^{estimated}} \quad \textit{Eq. 11}$$

As the algorithm is applied on a pixel per pixel basis, a statistical analysis on the ratio is made to remove outliers. Mean and standard deviation of the ratio are estimated and values out of three σ are removed.

3.2.2.10 Statistical analysis of the sensor radiometry

The last step consists in averaging the values of the ratio obtained for one acquisition and monitor it with time.

$$\overline{\Delta\rho} = mean\left(\frac{\rho_{TOA}^{Measured}}{\rho_{TOA}^{Simulated}}\right) \quad \textit{Eq. 12}$$

3.2.3 Auxiliary data

3.2.3.1 Thresholds

The following threshold has been defined:

Table 3-2: Threshold used to select data

Name	Threshold value
Maximum Cloud coverage	20%

3.2.3.2 BRDF climatology

In version 1 of the ATBD, the BRDF coefficients were available only for 5 years, introducing a limitation for using the methodology for years where BRDF coefficients were not available. An update of the data has been made, collecting data from the start of the collection 5 to end of 2016. Maps of the coefficients are illustrated hereafter. Each column represents the variability of the coefficients in the site along one year, each raw represents the data of a year.

Year 2000 starts on the raw 1, column 1 and ends on raw 1, column 46.

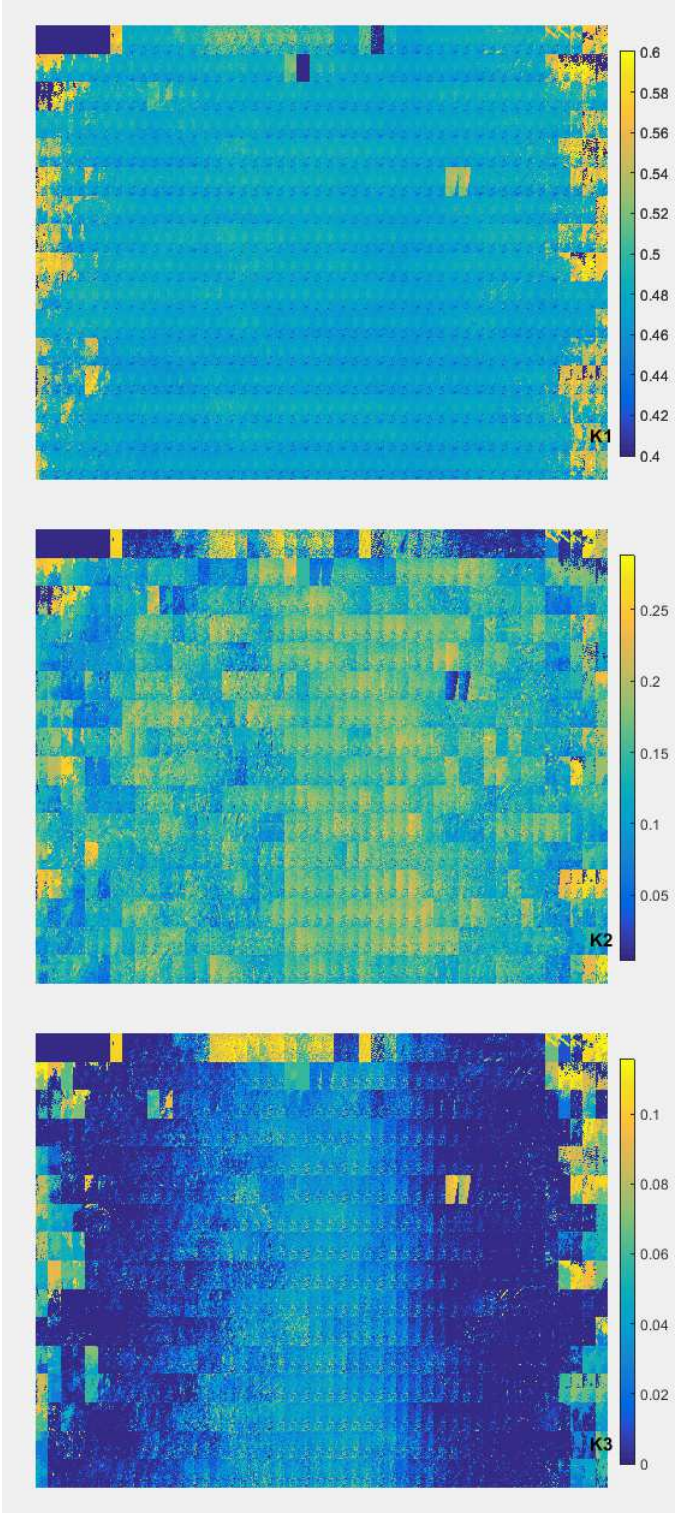

Figure 3-6: On the left, Maps of K1 (top), K2 (middle), and K3 (bottom) coefficients, and the map of mean value of each acquisition on the right

For each date, the mean of the coefficients is computed and represented here after.

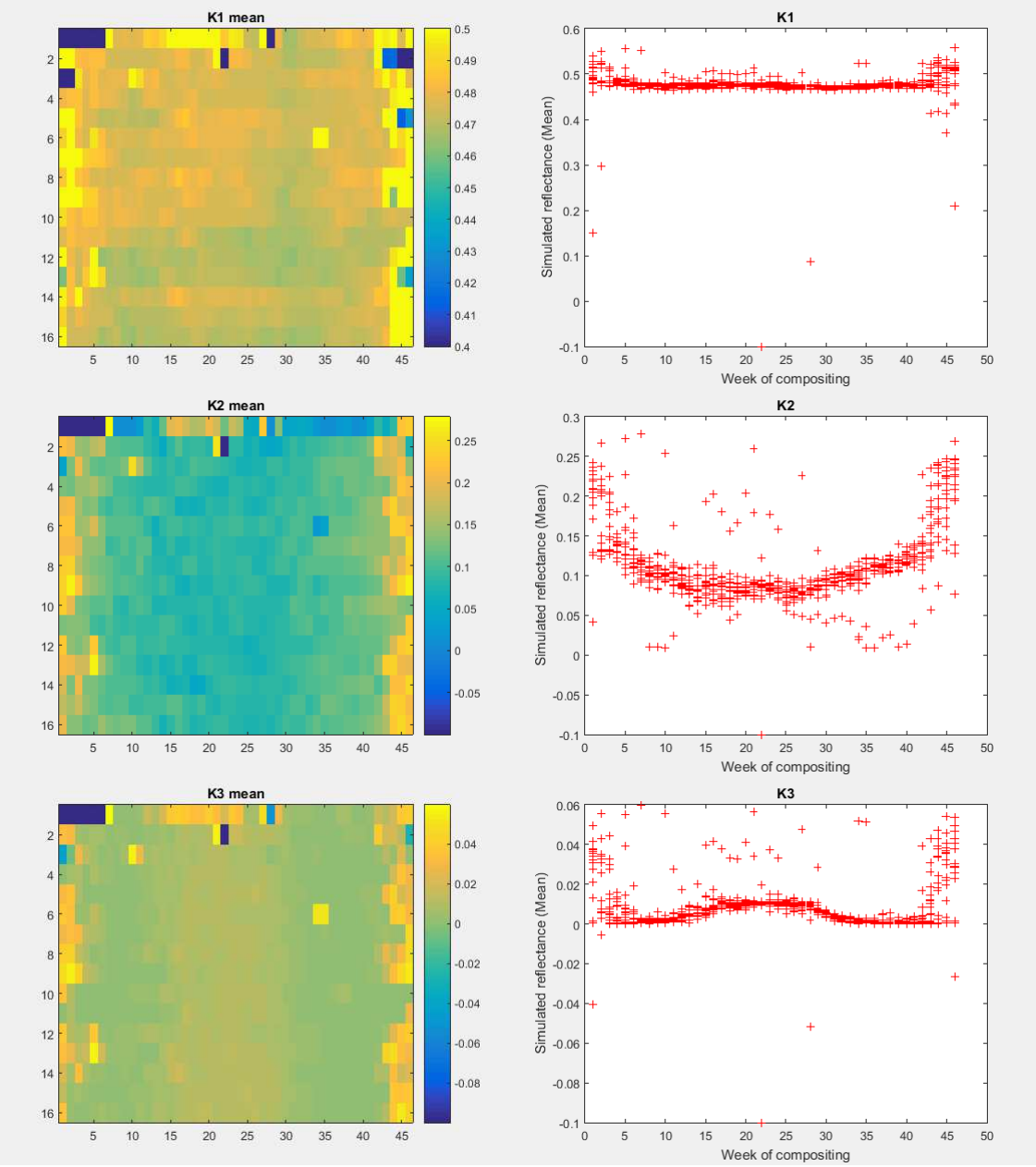

Figure 3-7: Maps of the spatial mean of coefficients, and their temporal variability vs the synthesis period

When looking at the temporal variability of the mean coefficients from one date to another one (Figure 3-7), it appears that for a same period, there is a certain variability around a mean value, and sometimes, values that are really different from the mean. These outliers are found either when the synthesis period is very cloudy, so there are only a few value available for the retrieval or if the clouds are not well detected and filtered and are present in the period used for the synthesis (see Figure 3-8 for instance), and also probably because there are some uncertainties coming from the atmospheric correction.

The following figures illustrate the variability of the K1 coefficients for three successive syntheses. We can observe that some residual clouds, not detected are present in the first two products, whereas the third one highlights a level of K0 different of the two previous one.

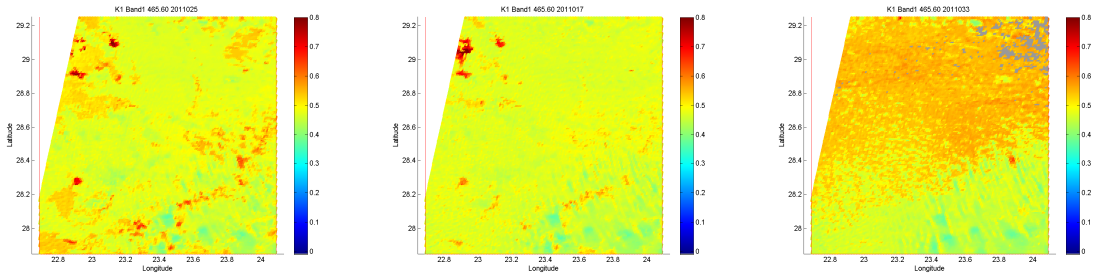

Figure 3-8: Variability of the K1 coefficient for three successive syntheses

With the assumption that the site is invariant, the BRDF coefficients for an identical period should be the same. MODIS repeat cycle is 16 days, the same as the period used for the coefficients retrieval.

If the variability of the coefficients is due to uncertainties on atmospheric corrections, a climatology of the three coefficients could be a solution to make the method independent of an update of the auxiliary data. 16 years of data (768 products) have been used to compute the climatology of the coefficients.

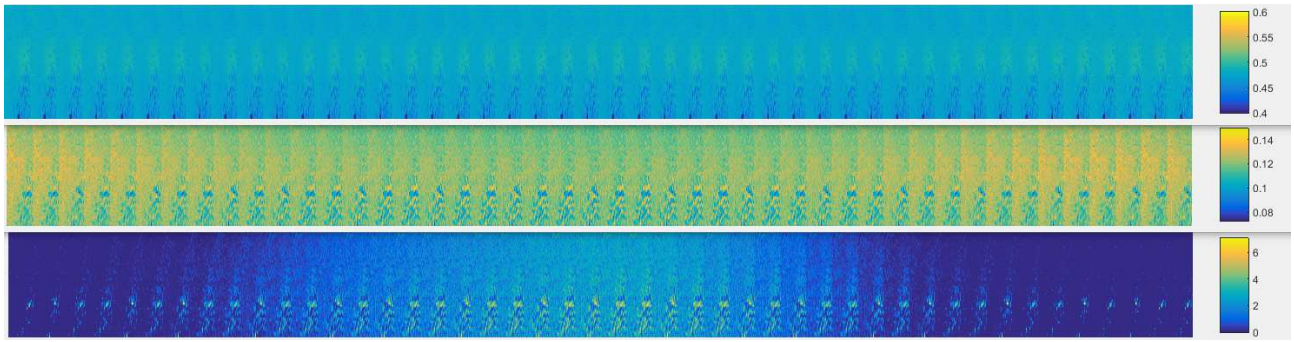

Figure 3-9: Climatology of K1, K2, K3(x10^{-3}) coefficients – 46 periods

3.2.4 Ancillary data

Water vapour content, ozone content and pressure are taken from the ERA interim datasets. ERA-Interim is a global atmospheric reanalysis from 1979 to present. Global atmospheric and surface parameters from 1 January 1979 to present, at T255 spectral resolution (~80 km) on 60 vertical levels are available. For this study, 6-hourly atmospheric fields on water vapour content, ozone content, and wind speed have been downloaded from 2001 to year 2016 from the ECMWF Data Server.

Table 3-3: Ancillary data needed in the DESERT method

Data	Source
Water vapour content	ECMWF ERA Interim
Ozone content	ECMWF ERA Interim
Pressure	ECMWF ERA Interim

4 Results

4.1 MERIS

The method has been applied to four years of MERIS data, [2006-2009]. Results are presented for each spectral band except band 11 in the figures below and statistics in Table 4-1.

ao and a1 represents the offset and the slope of the regression respectively. rmse is the root mean square error of the regression, Npt is the number of acquisitions retained in the synthesis, and r is the correlation coefficient.

Table 4-1: Statistics (DESERT_MAG_20191202-1336)

Wavelength (nm)	412	443	490	510	560	620	665
	Band 1	**Band 2**	**Band 3**	**Band 4**	**Band 5**	**Band 6**	**Band 7**
ao	0.9794	0.9986	1.0002	0.9915	1.0132	1.0066	1.0096
a1	-5.64e-05	-0.00023	7.485e-05	6.109e-05	0.0008082	0.001537	0.0011084
rmse	0.01915	0.022273	0.023418	0.022466	0.0201	0.016149	0.015577
Npt	403	403	403	403	403	403	403
r	-0.0032	-0.01203	0.003573	0.0029	0.0447	0.10579	0.079292

Wavelength (nm)	665	681.25	708.75	753.75	778.75	865	885	900
	Band 7	**Band 8**	**Band9**	**Band 10**	**Band 12**	**Band 13**	**Band 14**	**Band 15**
ao	1.0096	1.0038	0.9859	1.0075	1.0047	1.0020	0.9786	0.95933
a1	0.0011084	0.0010864	0.000145	0.0008607	0.000792	0.000741	0.00042271	-0.001190
rmse	0.015577	0.015354	0.0169	0.014716	0.014575	0.014095	0.014495	0.024747
Npt	403	403	403	403	403	403	403	403
r	0.079292	0.078851	0.0118	0.065245	0.06064	0.05868	0.0332	-0.053695

Band 15 which is located in water vapour absorption band is not considered in the analysis.

The evolution of the ratio is slow, or less, around 0.1 %. The offset is around 1, except in band 1, 9, 14.

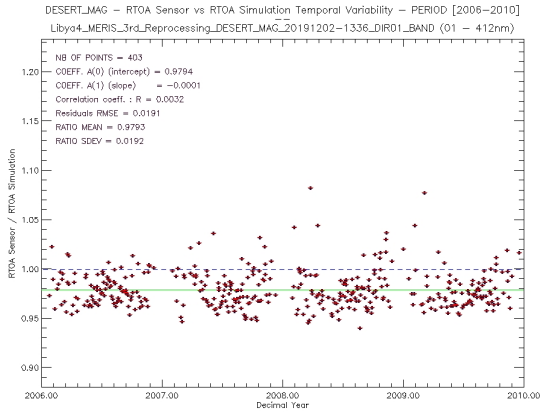

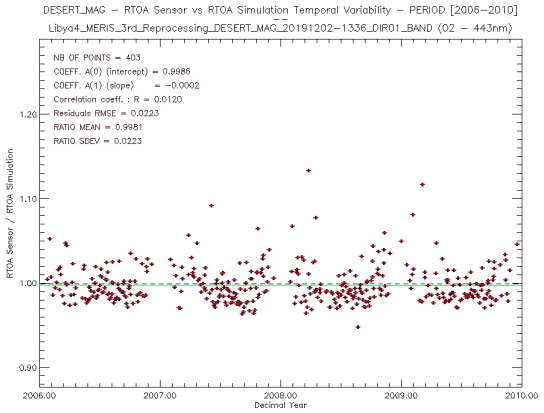

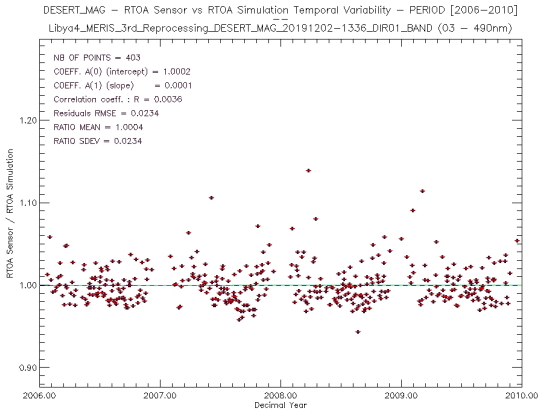

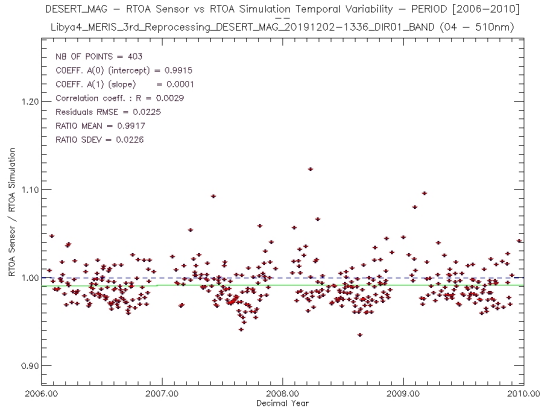

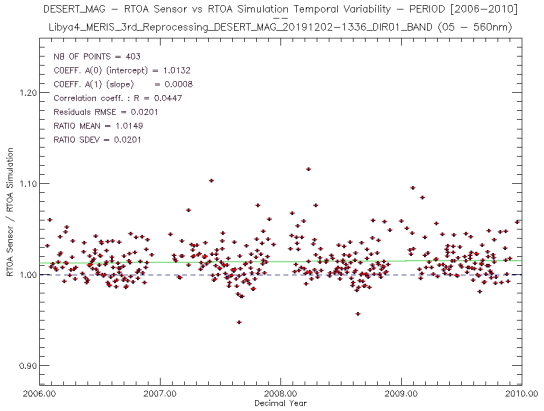

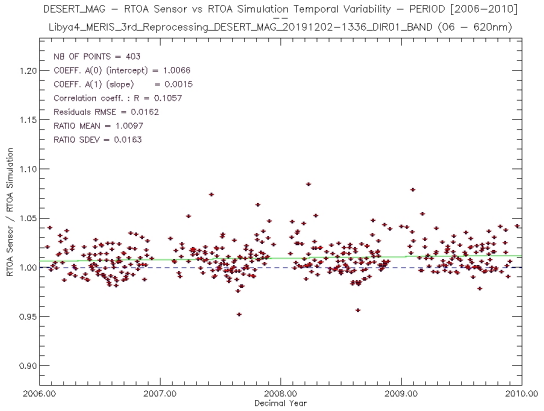

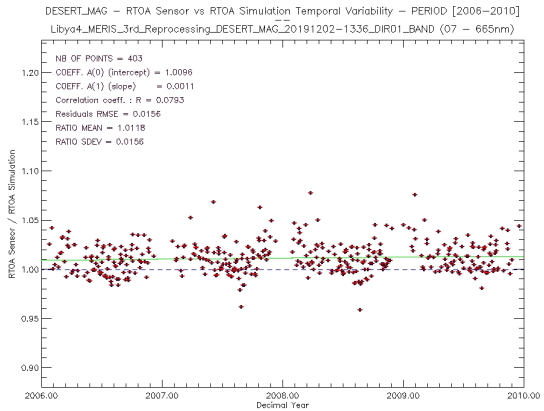

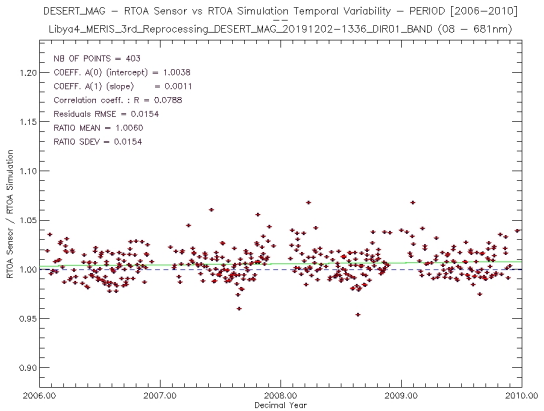

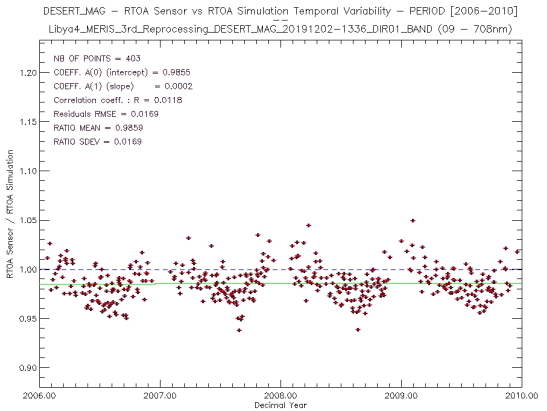

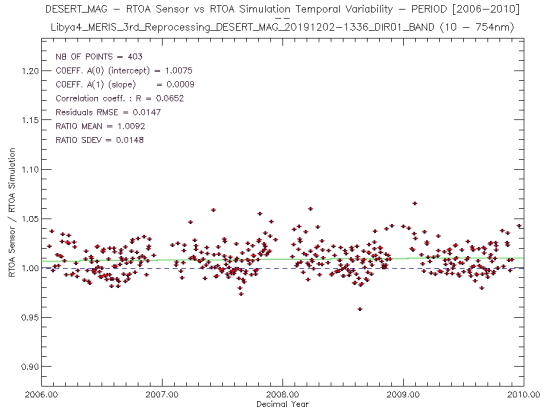

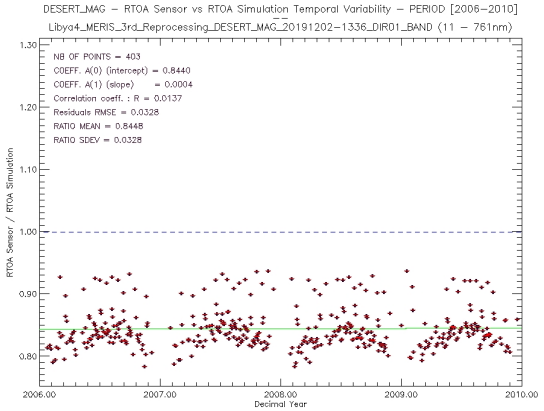

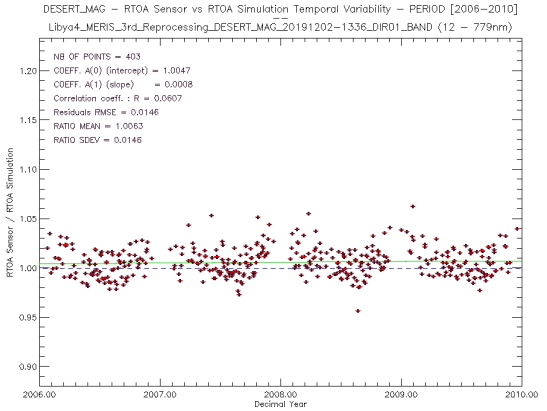

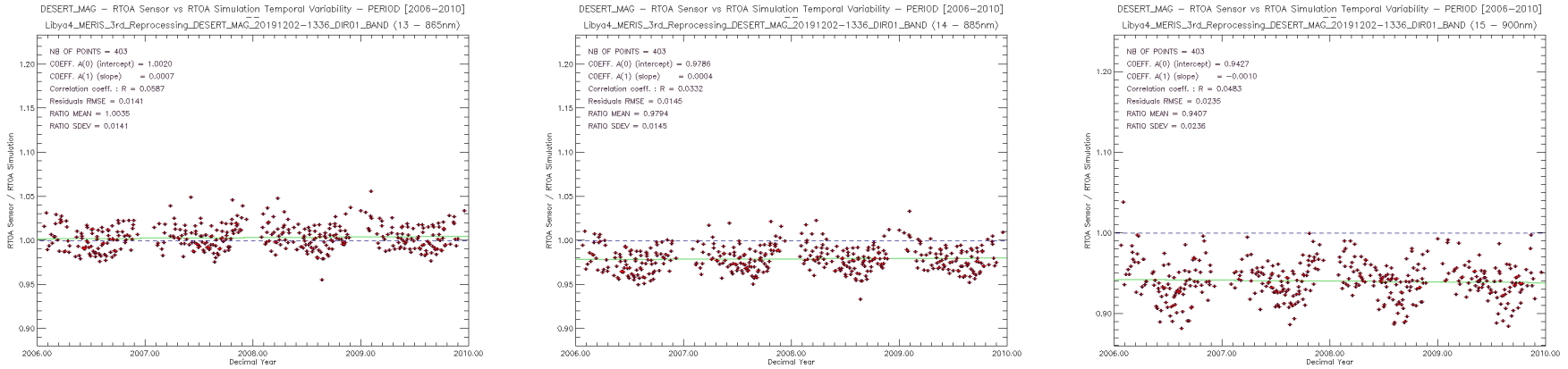

Figure 4-1: Measured/Simulated TOA reflectance ratio for MERIS band 1 to 15

5 Uncertainty budget

Main contributors of uncertainties introduced in our implementation could come from:

- Instrumental errors
  - Calibration errors.
- Geophysical uncertainties:
  - Gaseous absorption:
    - ozone amount : 5%
    - water vapour amount: 20%
  - Aerosol optical thickness: In our implementation, a mean invariant value of 0.2 is used with a desert aerosol model provided by 6S.
- Modelling
  - SMAC method: The performance of SMAC/6S atmospheric reflectance estimation has been evaluated by computing the root mean square error (rmse) and the maximum absolute or relative error with respect to the 6S reference for SMAC. More than 50.000 simulations including extreme variations of the input parameters have been made to get the following results. Accuracy is around 0.007 for blue bands (443 nm), 0.004 around 550 nm, 0.002 around 870 nm, and less than 0.001 in the SWIR (Berthelot, 2001).
  - BRDF model: error on BRDF coefficients is not estimated directly but through the validation of the albedo. MODIS team reports that the accuracy of the high quality MODIS operational albedos at 500m is well less than 5% albedo at the majority of the validation sites studied thus far and even those albedo values with low quality flags have been found to be primarily within 10% of the field data.
  - Spectral resampling: the use of hyperspectral spectrum allowed to remove extrapolations between 400 nm and 2500 nm and thus errors in the spectral bands located before the first MODIS band and the last one. The use of the spectrum decreases systematic BRF errors observed on MERIS for instance where systematic errors decreases to 1 or 2%
- Spectral band knowledge used for spectral interpolation and SMAC coefficients estimation
- Quality of geometrical coupling between measurements and MODIS products. An error of geolocation of 1 pixel could change the estimate the BRDF, as the site is not homogeneous at this scale.

- End of the document -